

4 Substrate and interface effects

In the previous chapter I discussed the formation of quantum well states in a variety of systems, and showed that, from a general point of view, the binding energies and the development of the QWS with coverage only depends on the nature of the overlayer material. The exact details of growth do, however, depend on the substrate and interface properties. Furthermore, the formation of magic height islands of Pb strongly depends on the substrate; on the Si(111) $\sqrt{3}$ surface 6 ML high islands are preferred, on the Si(111)7x7 surface 8 ML high islands, on graphite only the even layer heights below 9 ML are formed, and on Cu(111) a variety of heights. In this chapter two kinds of substrate/interface effects will be discussed; the influence of the interface *atomic* structure, and the influence of the interface *electronic* structure. In some instances, both effects can have similar results and are heavily intertwined, therefore they will sometimes be treated simultaneously, depending on the studied system.

4.1 The influence of lattice mismatch and relaxation on QWS

The exact growth of metal overlayers can be of substantial influence on the formation of quantum well states. In Chapter 3 it was shown that from a coverage of approximate 7 ML, indium grows in a layer-by-layer fashion, both on Si(100) and on Si(111). Although entirely correct, this statement only gives information about how the next deposited layer will form with respect to the previous one. That a major difference does exist between the growth mode on the two different substrates is clear from Figure 4.1, where LEED patterns for a 10 ML thick film of indium on Si(111) (left) and a film of identical thickness on Si(100) (right) are shown. The most striking distinction between the two patterns lies in the number of spots; 6 for the layer on Si(111) and 12 for the layer on Si(100).

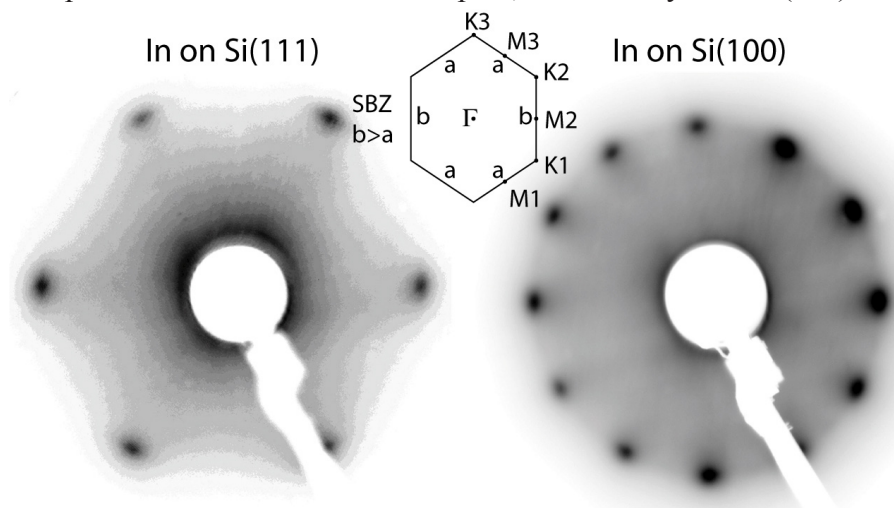


Figure 4.1: LEED patterns for a 10 ML film of In on Si(111) (left) and on Si(100) (right). (inset) SBZ for a *bct* lattice with an exaggerated difference between *a* and *b*. The lines in the left image are due to the enhancement of contrast.

From the comparison of QWS energies to DFT results, and from the hexagonal LEED pattern, it can be concluded that on both substrates the layers grow in the [111] direction. Due to the fact that the Si(100) surface consists of two domains that are rotated 90° to each other, the indium overlayer will also grow in two domains. This explains why there are 12 diffraction spots for In/Si(100) and 6 for In/Si(111). From the sharpness of the spots the good crystalline quality of the layer, which was expected from the well defined QWS shown in Figures 3.17 and 3.21, can be confirmed.

Bulk indium has a body-centred tetragonal crystal structure, which means that when cutting to obtain a [111] plane, the surface Brillouin zone has the shape shown in the inset in Figure 4.1, where for clarity the distortion from the *fcc* hexagon is exaggerated. In real space the distance a is 3.8% larger than the interatomic distance b , in the SBZ this is inverted. This distortion of the perfect hexagon should also show up in LEED; it should look elongated in one direction. For the LEED images presented in Figure 4.1, this elongation is not directly visible. A numerical analysis of the LEED pattern was carried out using the following routine: along a horizontal axis, cutting exactly through two spots, an intensity trace is extracted from the image. The peaks in this spectrum are then fitted with a Gaussian function in order to deduce the exact peak positions, and in reciprocal space the spacing. The use of spacing between two spots in the subsequent analysis, instead of their absolute position, reduces the influence of errors produced by a slight angular misalignment of the sample in front of the LEED instrument. The image is then rotated to obtain the next two spots along the horizontal axis, taking extra precaution not to distort the image in the process, and the analysis is repeated. In this way, for In/Si(111) three distances, and for In/Si(100) six distances are obtained. Repeating this procedure for several coverages results in a spot distance versus coverage plot as shown in Figure 4.2. The upper plot is for In/Si(100), wherein the different symbols indicate the two domains. The lower plot is for In/Si(111); in both plots, lines connect those geometrical orientations that belong together.

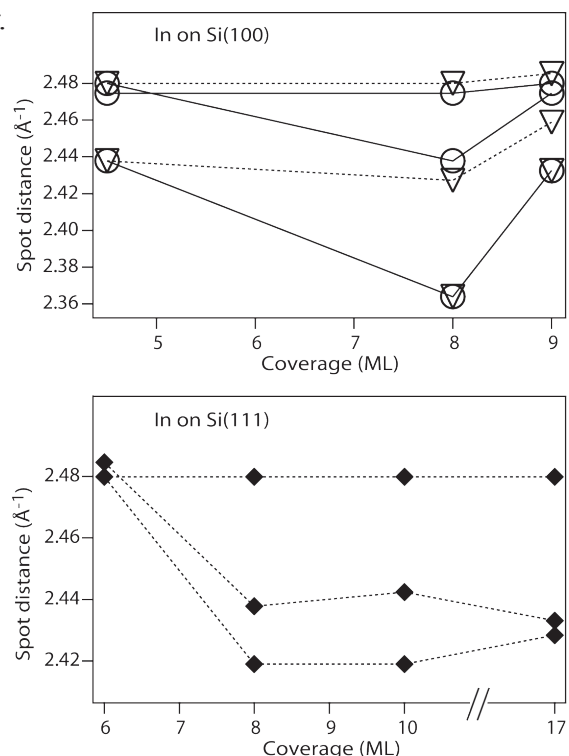


Figure 4.2: Spot distance derived from LEED patterns as described in the text as a function of coverage for In on Si(100) (top) and In on Si(111) (bottom). Similar symbols belong to the same domain, the lines connect those geometrical orientations with respect to the substrate that belong together.

From the fact that for the indium films on Si(111), the spot distances for a coverage of 6 ML are the same in all three directions, it can be concluded that the In layer initially grows in a face-centred cubic structure. This, for indium uncommon¹, lattice structure is induced by the *fcc* structure of the silicon substrate. For higher coverages, the layer asymmetrically relaxes towards a body-centred tetragonal crystal structure, indicated by the observation that two distances in reciprocal space are shorter than the other. For the 17 ML thick layer, the difference between the long and short axis is approximately 2%. Considering that the layer will not be fully relaxed towards the bulk lattice at this film thickness, this value is in good agreement with expectations. That the strain imposed on the thinner layers by the substrate has a large impact follows from Figure 3.21. In the layers with an *fcc* structure, no clear QWS are formed, and in the energy versus momentum image in Figure 3.22 only a broad non-dispersing feature is observed just above the silicon valence band maximum. In a recent STM study² it was shown that the underlying Si(111)7x7 surface could still be imaged through indium islands with a height of 7 ML. Because STM is a method in which electrons with k_{\parallel} over a wide range contribute, structural information buried below a metal layer normally cannot be obtained. This limitation is also valid for thin metal layers, where an electron can maintain its phase information over the distance travelled through the film. Because the electronic state observed for *fcc* indium films is non-dispersing, it can provide a perfect pathway through which the interface structure is visible, although the STM integrates electrons that are emitted over a broad angular range. It is crucial in this interpretation that the tip, when the image mode is used, extracts or injects electrons with a constant energy. If the same state has a constant energy over a broad k_{\parallel} range (and therefore angular range), the emitted electrons within this range interfere constructively to form a complete image. This interpretation of the STM data is supported by the fact that for indium films thicker than 7 ML, the In/Si interface is no longer visible. In the photoemission study presented in Figure 3.21, this is confirmed by the formation of QWS with a free-electron-like dispersion. This means that electrons with different in-plane momentum which are extracted with the STM, do not necessarily belong to the same state and cannot interfere constructively to form an image of the substrate.

From the general trend in the spacing of the LEED spots as a function of coverage it is clear that the growth mode of indium on Si(100) differs from that on Si(111). First, on Si(100) not all spot distances are identical for thinner layers, suggesting that the initial growth is *bct* and not *fcc* like. The asymmetry in spot distances remains similar for higher coverages, indicating that the thinner layers are relaxed in manner comparable to the thicker ones. For In/Si(111) it was seen in the LEED pattern, that in the *bct* growth region, one distance is larger than the two others; this would also be expected from the bulk lattice structure. Measurements for In/Si(100) yield a different result; the asymmetry for the two different domains is opposite to each other. The triangular markers,

1 S.I. Simak et al. Phys. Rev. Lett. 85, 142 (2000).

2 I.B. Altfeder et al. Phys. Rev. Lett. 92, 226404 (2004).

from what is termed domain 1, show one distance being larger than the others. On the other hand, domain 2, represented by the diamonds, shows one spot spacing being shorter than the other two. Addition of these two domains rotated 90° with respect to each other results in the oval shape of the LEED pattern in the right image of Figure 4.1. The variations in distance and the general oval shape of the LEED pattern are also confirmed by the fact that, in order to rotate the image to horizontally align the next spots, variations in the rotation angle of as much as 3° are needed. These variations cancel each other, so that a half rotation is exactly 180° . From a comparison to LEED images obtained for the clean Si(100) substrate directly before indium deposition, it can be concluded that the “odd” distance (i.e. the distance shorter/longer than the other two) is aligned parallel to the dimer rows. This alignment, perpendicular to the dimers, is the only way that the square symmetry of the substrate can be partly matched by the *bct* symmetry of the overlayer. The asymmetry between the growth on the different substrate domains is induced by the 4×2 low temperature reconstruction of Si(100)³.

The observation of QWS is not influenced by the growth of two different domains of indium overlayers. In the centre of the surface Brillouin zone the Γ -M direction of domain 1 and the Γ -K direction of domain 2 will exactly overlap. The deviation between the energy bands in the two directions, which can only be probed simultaneously in photoemission, will increase for larger k_{\parallel} values. Figure 4.3 shows a comparison between an energy versus angle image obtained towards the edge of the SBZ in the Γ -M direction for 10 ML of In/Si(111) (left), and for the same emission angle from 9 ML of indium on Si(100) (right). In the image obtained for In/Si(111), the features are significantly sharper than for In/Si(100); this can be confirmed from the energy cuts through the image (top), taken at the point where the topmost QWS crosses the Fermi level,

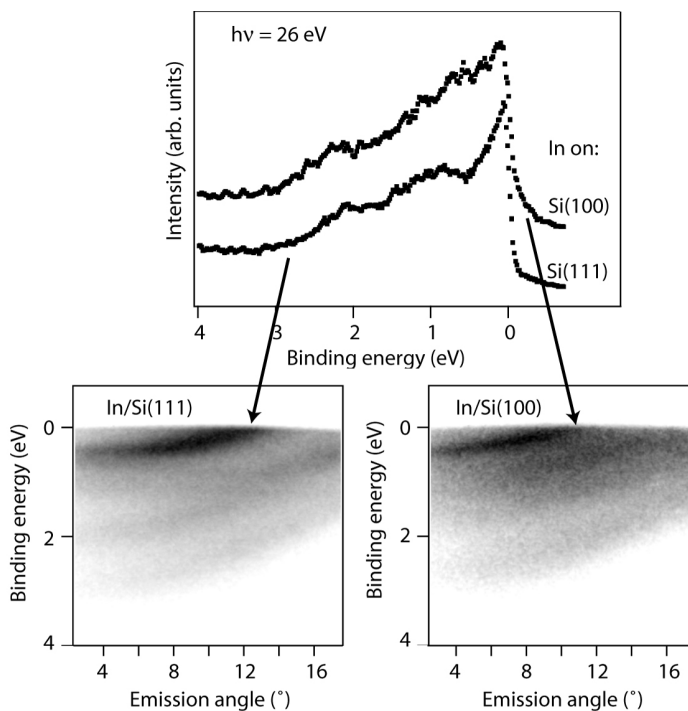


Figure 4.3: Off-normal emission images for In/Si(111) (left) and In/Si(100) (right) at a photon energy of 26 eV. The arrows indicate where the spectra in the upper part of the figure are extracted. Note the difference in sharpness of the features. The images have been inverted for clarity, darker colours indicate a higher photoemission intensity.

indicated by the arrows. For the In/Si(111) EDC, three individual peaks can be resolved, whereas for In/Si(100) the peaks seem to be twins and can hardly be resolved. Considering the fact that both layers are relaxed towards a *bct* lattice structure, the difference in peak width is due to the mixture of domains. Because the different domains originate from the two domains in the substrate, suppressing the two-domain growth of indium on Si(100) would seem possible by using the single domain Si(100) substrate with a 4° miscut. A separate experiment with such a substrate was carried out; unfortunately, due to the large influence of the step edges the formation of single domain In layers on Si(100) was not possible. From the LEED pattern it follows that the indium overlayer does grow in a single domain, the spots are, however, in all directions very broad. That the crystalline structure of the layer is not well established is confirmed by our photoemission measurements, where no indium features are present in the valence band of these layers, apart from the Fermi edge.

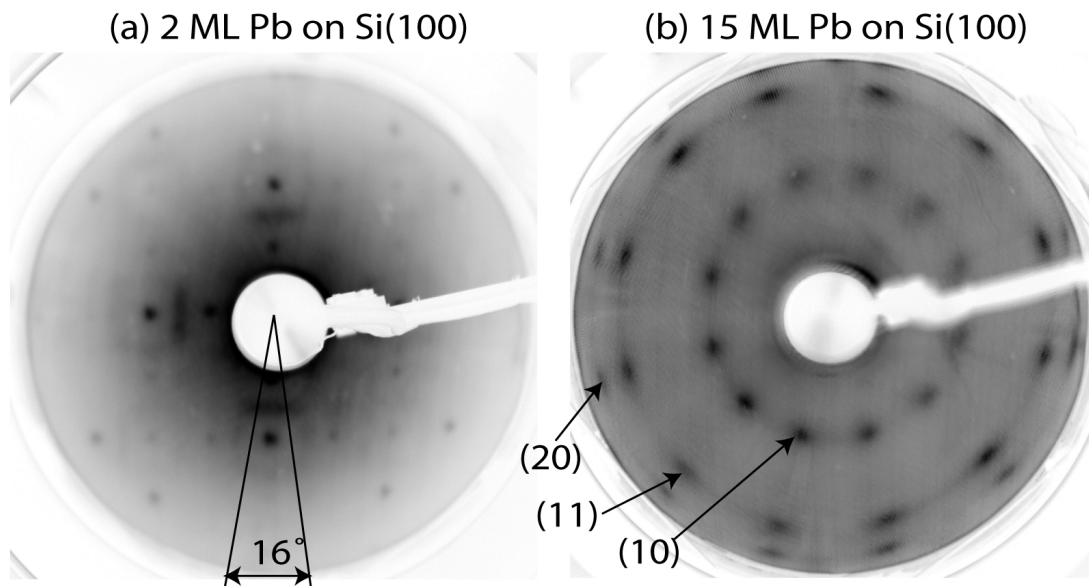


Figure 4.4: LEED patterns for (a) 2 ML Pb on Si(100) obtained at a electron energy of 80 eV, and (b) 15 ML of Pb on Si(100) obtained at 105 eV

That the strain induced by the substrate can have a profound influence on the formation of QWS is also obvious for Pb films on Si(100). Figure 4.4(a) shows the LEED pattern obtained after the deposition of 2 ML of Pb on Si(100), obtained at an electron energy of 80 eV. On the inside of the sharp spots from the square silicon substrate lattice, an elongated spot can be observed that is not present for clean Si(100). Upon closer inspection it is clear that this “dash” is actually composed of two separate spots. These spots can be assigned to a square lattice with an 8° rotation compared to the Si(100) lattice, suggesting the formation of an epitaxial Pb(100) layer induced by the symmetry of the substrate. This layer should also leave its signature in ARPES, in that a QWS should show up at a binding energy of approximately 1.8 eV as predicted by a theoretical treatment of this system⁴. Figure 4.5 shows a comparison between a 5° off-normal emission photoemission

⁴ D. Yu, M. Scheffler, and M. Persson, unpublished.

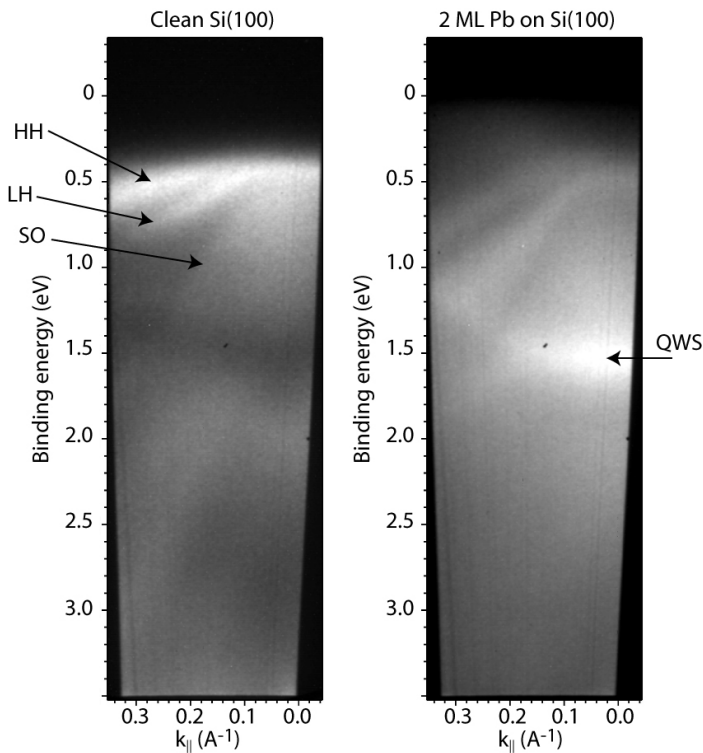


Figure 4.5: (left) Photoemission image for clean Si(100) at a photon energy of 24 eV with the heavy-hole (HH) light-hole (LH) and split-off (SO) bands indicated. (right) Image obtained with the same parameters for 2 ML of Pb on Si(100), with the QWS indicated.

image for clean Si(100) and the 2 ML thick Pb(100) film formed on this substrate. The images were obtained with the dispersing angle along the horizontal direction of Figure 4.4(a). For the clean substrate, the heavy-hole (HH), light-hole (LH), and split-off (SO) bands⁵ can be identified, and are marked accordingly. At a binding energy of 1.5 eV, a gap is observed for emission from the clean Si(100); this coincides nicely with the region where, from electronic structure calculations⁶, a gap state can be expected for a Si(100)4x2 substrate. After Pb deposition, an intense upward dispersing feature is formed exactly in this gap, which does not disperse with photon energy. Combining this information with its absence on the clean substrate leads to the conclusion that this feature is a quantum well state. The binding energy of this state is slightly lower than predicted for a freestanding Pb(100) film of 2 ML thickness⁴. However, especially for such thin layers the discrepancy between calculation and measurement is expected to be, and has already been proven to be large when the substrate influence is not negligible. In Figure 3.32 this is illustrated by the discrepancy between the measured and calculated QWS binding energies. Emission from the silicon bands remains visible underneath the Pb overlayer, the intensity distribution has, however, changed, with higher intensities in regions close to the Pb QWS. This enhancement of the substrate bands due to the presence of a QWS in the overlayer material, will in Section 4.4 be shown to be a general property of metallic quantum wells on semiconductor substrates.

For higher coverages of Pb on Si(100), QWS are no longer observed; only a broad feature, dispersing with photon energy exactly like the bulk band, is visible. This feature is comparable to observations for the unannealed Pb films on Cu(111) and Si(111) in Chapter 3, and is due

5 F. Hermann, *Rev. Mod. Phys.* **30**, 102 (1958).

6 J.E. Northrup, *Phys. Rev. B* **47**, 10032 (1993).

to disorder in the film. As discussed in Chapter 1, the QWS wave function is composed of the rapidly oscillating Bloch wavefunction derived from the Pb atom spacing, modulated by the slowly varying QWS envelope function. This QWS envelope function can only exist if a standing electron wave is formed, which in turn depends on coherent backscattering at the interface and phase information loss-free travel through the layer. That this is not possible for the Pb layers on Si(100) thicker than 2 ML follows from an analysis of the LEED image obtained for these films shown in Figure 4.4(b). The third layer no longer grows in a square lattice, but in the hexagonal structure of a Pb(111) layer. The two domains of the Si(100) substrate are responsible for the fact that 12 spots can be observed. This LEED pattern has been obtained with an electron energy of 105 eV; at this energy also the higher order diffraction spots are visible (indicated in the image are the (10), (11), and (20) spots for one domain). Due to the 90° rotation between the domains, the (11) and (20) spots from different domains almost overlap. Compared to Pb/Si(111)7x7 (Figure 3.12(b)) the spots are relatively sharp, and in that system QWS are formed, therefore the limiting factor is not in the overall crystal structure of the overlayer. For coverages of approximately 4 ML, a combination of the square lattice from Figure 4.4(a) and the hexagonal lattice from Figure 4.4(b) is observed. This suggests that the 2 ML thick Pb(100) layer survives underneath the Pb(111) film for higher coverages. This change in growth direction is devastating for the possibility of coherent backscattering at the interface, therefore no QWS can form and only the bulk-like band dispersion shows up.

The growth mode of Pb on Si(100) can be explained by a combination of two effects, i.e. the strain induced by the substrate, and electronic growth effects comparable to results in the second part of Chapter 3. That the initial growth is in the (100) direction is obviously due to the symmetry of the substrate, but that the 2 ML thick layer is formed and survives under thicker films is due to energy minimization effects. The total energy per unit cell of a free-standing 2 ML thick Pb(100) layer is about one third lower than the total energy per unit cell of thicker Pb(100) films⁴, and almost half of that for a 3 ML thick layer. The formation of a Pb(111) film on a Si(100) substrate involves a considerable amount of strain in the overlayer, which increases the total energy of the layer. Although the total energy of Pb(111) layers⁷ is much lower than that of Pb(100) layers over the full studied range, the extra energy due to strain shifts the advantage for 2 ML thick films in the direction of the Pb(100) structure. Due to the large energy increase for the formation of a 3 ML thick Pb(100) layer, the growth direction then suddenly changes to (111). The 2 ML film is stabilised, just like the preferred Pb layers discussed in Section 3.2, due to quantum size effects and will survive. In this context it is also important that for a 2 ML thick film the QWS is located exactly inside the substrate band gap at 1.5 eV. This enhances the confinement conditions, and therefore the influence of quantum size effects on the total energy of the film. For higher coverages the QWS move outside this bandgap, and the confinement is less effective; for these layers the stabilising influence of QSE is therefore reduced.

7 C.M. Wei and M.Y. Chou, Phys.Rev. B **66**, 233408 (2002).

4.2 Influence of the interface atomic structure and the substrate bandgap

The importance of the atomic structure of the interface on the formation of quantum well states was emphasized several times in this thesis. In the previous section the absence of QWS in thicker layers of Pb on Si(100) was explained by the change of layer structure, its effect on the formation of standing electron waves. Figure 1.10 in Section 1.4 gives a graphic representation of the three main processes that can occur when an electron approaches an interface, or any other potential barrier. These are: transmission of the electron across the interface, incoherent backscattering with loss of phase information, and coherent backscattering resulting in the possible formation of standing electron waves. Roughness at the metal-vacuum interface is minimal due to the smoothing influence of quantum size effects as described in Section 3.2, and due to surface energy minimization; therefore this interface can be regarded as ideal. This means that incoherent backscattering is negligible at this interface. Apart from the charge spilling due to electron tunnelling, which is incorporated in the phase shift, no transmission of electrons across the metal vacuum interface is expected. Hence only the interface between the metal film and the substrate can limit the formation of QWS, assuming a good crystalline quality of the rest of the layer.

The difference in the formation of QWS in Pb films deposited on Si(111)7x7 and Si(111) $\sqrt{3}$, provides a good example for the influence of the interface atomic structure. A major advantage in this comparison is that the constituents remain the same, the only difference between the two systems being the interface structure. This difference in interface reconstruction is known to influence the formation of stable island heights⁸ (6 ML on Si(111) $\sqrt{3}$ and 8 ML on Si(111)7x7). Experiments leading to these conclusions were performed at a temperature of 195 K, which is approximately 100 degrees higher than the temperature used in the experiments presented here, and comparable to the mild anneal used on the Pb films deposited on Si(111)7x7 presented in Chapter 3. As will be shown below, at these elevated temperatures it can be expected that the interface structure has changed.

The 7x7 reconstruction at the interface can still be observed in STM⁹, through Pb layers as thick as 100 Å deposited on a clean Si(111)7x7 substrate. This means that the assumption that the 7x7 reconstruction survives underneath the Pb film^{10, 11} is correct. The same assumption might be done for the $\sqrt{3}\times\sqrt{3}$ surface reconstruction, but this has neither been confirmed nor refuted. Currently, expert opinion on this issue is that the Pb induced $\sqrt{3}\times\sqrt{3}$ reconstruction layer will survive at the low temperatures used for deposition in the studies presented here, and at higher temperatures

8 V. Yeh, L. Berbil-Bautista, C.Z. Wang, K.M. Ho, and M.C. Tringides, *Phys. Rev. Lett.* **85**, 5158, (2001).

9 I.B. Altfeder, D.M. Chen, and K.A. Matveev, *Phys. Rev. Lett.* **80**, 4895 (1998).

10 H. H. Weitering, D. R. Heslinga, and T. Hibma, *Phys. Rev.B* **45**, 5991 (1992).

11 F. Gray et al., *J. Phys. (Paris)* **50**, 7181 (1989).

will be incorporated into the overlayer formed on this surface¹². A comparison of Figure 3.7 (left) and Figure 3.9 gives a good indication of the influence of the different interfaces on the formation of QWS. On Si(111)7x7 the peaks due to the QWS are relatively broad and not very intense, and a large contribution from the bulk-like feature introduced in Chapter 3 can be identified. After deposition of Pb on the Si(111) $\sqrt{3}$ surface, on the other hand, the QWS are very sharp and intense and the contribution of the bulk-like feature is limited. The difference in QWS width can be partly explained by the fact that, for deposition on the 7x7 substrate, a mixture of adjacent layer heights is grown, leading to QWS peaks that are actually composed of contributions of states from several heights that slightly overlap. This does not necessarily lead to a broadening of the measured photoemission peaks, as indicated by the growth of Al on graphite, where individual QWS can still be resolved, although a mixture of several adjacent heights is present (Figure 3.27). Hence, the broadening of the QWS in Pb/Si(111)7x7 relative to those in Pb/Si(111) $\sqrt{3}$ cannot be solely attributed to the rough growth front of the former.

For both Pb/Si(111) systems, the part of the layer that is not directly influenced by the substrate is the same. Electrons travelling through this region experience the periodic potential of the Pb ions, resulting in the Bloch wave characteristic for the Pb atomic spacing. When the electron approaches the interface, the difference between the systems becomes relevant. First, consider the $\sqrt{3}\times\sqrt{3}$ reconstructed interface. The exact local structure of this interface is not known; it most likely consists of a mixture of phases from the “Devil’s staircase”¹³ of phases for this reconstruction. It is certain that the substrate is very smooth over extended regions before deposition, and there is no reason to assume that this changes in the course of layer formation. The intermediate interface layer is matched to both the atomic structure of the Si substrate and that of the Pb overlayer. An electron wave crossing this interface will thus not experience any incoherent backscattering, and the resulting possibilities are transmission across the interface and coherent backscattering. Transmission is only possible when there are allowed states in the substrate. Due to a Schottky barrier height (SBH) Φ_{SB} of 0.93 eV¹⁴ the valence band maximum (VBM) of Si(111) is situated at 0.32 eV below the Fermi level; the corresponding situation for a p-type semiconductor substrate is schematically depicted in Figure 4.6¹⁵. Above the VBM, there are no allowed states in the substrate, and the impinging electrons experience a potential barrier. This potential step causes backscattering of the electron without altering its phase information, and a standing electron wave can form. Because there are no additional scattering mechanisms in this energy region, the confinement of the electrons is almost perfect and the QWS peaks measured in ARPES will be very sharp. At binding energies larger than the Si VBM (> 0.32 eV), there is a large number of states that the electrons approaching from the Pb overlayer can couple to. The potential step in this

12 M.C. Tringides, private communication.

13 M. Hupalo, J. Schmalian, and M. C. Tringides, *Phys. Rev. Lett.* **90**, 216106 (2003).

14 D.R. Heslinga et al. *Phys. Rev. Lett.* **64**, 1589 (1990).

15 H. Lüth. *Surfaces and Interfaces of Solids*, volume 15 of Springer Series in Surface Sciences. Springer-Verlag, Heidelberg, (1993).

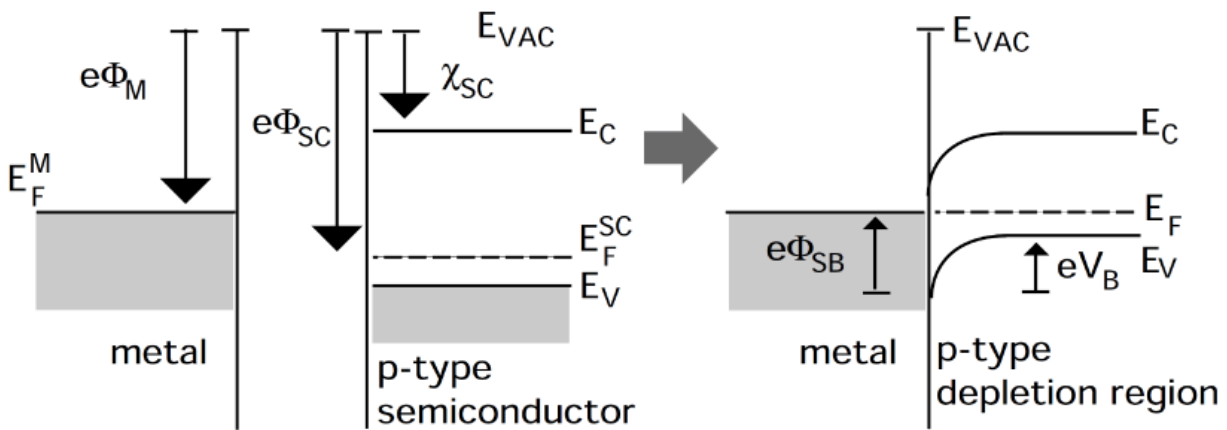


Figure 4.6: Schematic diagram of band bending before and after metal semiconductor contact according to the Schottky model for a low-workfunction metal and p-type semiconductor. Figure from Lüth¹⁵.

energy region is therefore small, and transmission across the interface prevails and no QWS are formed. This effect is illustrated by the position of the QWS in Figure 3.10; no states are formed outside the Si bandgap.

For Pb deposited on the Si(111)7x7 substrate, the situation is different due to the survival of the 7x7 reconstruction. For this reconstruction, large triangular domains separated by dimer rows are characteristic; where these rows meet, large corner holes are formed¹⁶ (Figure 4.7). Deposition of Pb layers on this surface results in a large number of buried scatterers and furthermore a generally rough interface. Electron waves approaching this interface outside of the flat triangular domains of the 7x7 reconstruction are backscattered incoherently, and do not contribute to the formation of QWS. Within the triangular domains, the situation is comparable to the Si(111) $\sqrt{3}$ reconstructed substrate. This means that inside the Si bandgap, the electrons experience a potential barrier, while outside this gap they can traverse the interface. However, the position of the VBM is different

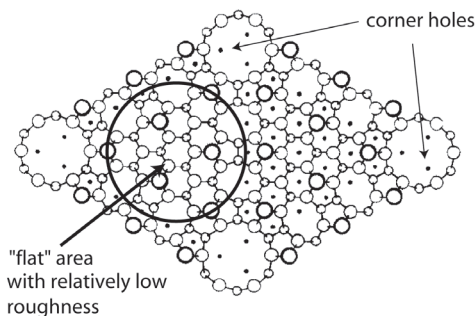


Figure 4.7: Structure of the Si(111)7x7 reconstruction with the corner holes indicated. In the “flat” area there is only limited roughness due to the adatoms. Figure from Takayanagi¹⁶.

in this case because of a different Schottky barrier height (0.70 eV^{14}); the Si VBM is therefore located at approximately 0.55 eV , and the energy region where QWS can form is slightly larger. The incoherently scattered electrons still have a Bloch wavelength characteristic for Pb, and will show up in the spectra as the feature reminiscent of bulk Pb (left part of Figure 3.7). In order to further confirm the origin of this state, spectra have been recorded as a function of coverage at a photon energy ($h\nu = 28 \text{ eV}$) where this feature is very prominent, with the resulting data being shown in Figure 4.8. From the absence of change, apart from a continuous increase in intensity, I conclude that the feature is not from a confined state, but from the incoherently backscattered electrons, the number of which increases with coverage. In a previous measurement¹⁷ of Pb on Si(111)7x7 this broad feature was mistakenly interpreted as a superposition of several QWS. The strong dispersion with photon energy was explained by the strong matrix element effects in Pb, causing only the QWS to be visible where there is a direct transition in photoemission for bulk Pb. Although I have shown in Chapter 3 that these matrix element effects are indeed stronger in Pb than in other metal overlayers (In and Al), and that QWS in a certain energy range are best probed when this direct transition occurs, Pb layers on Cu(111) and graphite provide a strong argument against interpreting the bulk like feature as a superposition of QWS. From Figure 3.3(b) and Figure 3.13 it is clear that, using one single photon energy (24 eV), QWS can be probed up to a binding energy of at least 3 eV .

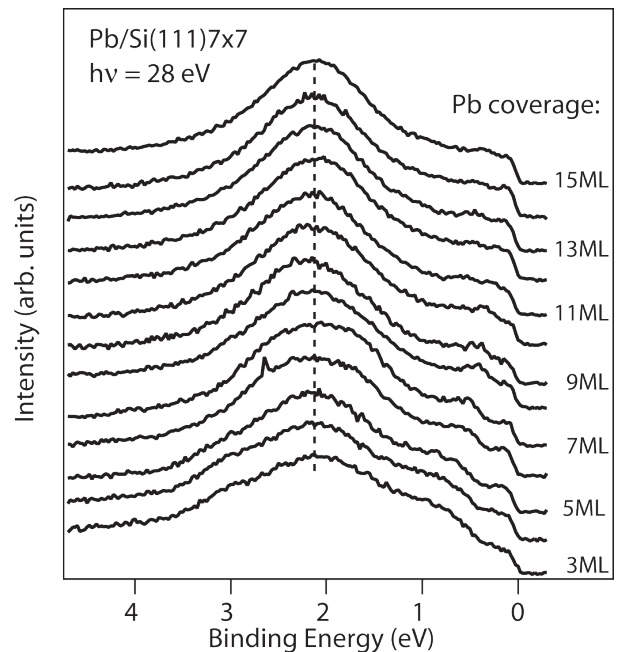


Figure 4.8: Valence level spectra as a function of coverage for Pb on Si(111)7x7 deposited at 100 K recorded at normal emission at a photon energy of 28 eV . Note the absence of features that change with coverage.

In Pb/Si(111) no QWS are formed at these binding energies due to the absence of a confinement barrier outside the Si bandgap, this being the only reason that they are not observed in the photoemission data. The assignment of this bulk-like feature as QWS can lead to a possible misinterpretation of other observations in Pb/Si(111) as will be discussed in Chapter 5.

After annealing, the abovementioned bulk-like feature disappears (right part of Figure 3.7), and only the bulk transition envelope function of the QWS remains. The annealing of the sample smoothens the interface, and therefore strongly reduces the number of sites responsible for incoherent backscattering of the electrons. In order to minimize the strain, the interface forms a superlattice with a periodicity of $1/\Delta a$, where Δa is the percentage difference between the two interatomic distances (in this case resulting in a periodicity of 11 atoms). Apart from this, annealing also causes the layers to rearrange towards a single height, observable in the formation of a single QW peak. Altfeder *et al.* have performed atomic position resolved scanning tunnelling spectroscopy (STS) experiments on both the as-deposited⁹, and a system resembling the annealed Pb layers on Si(111)7x7¹⁸, with striking differences. For the annealed Pb layers, there is an energy shift of the QWS of 60 meV for a 7 ML thick layer and of 30 meV for a 19 ML thick layer. This shift represents the energy difference between the measured QWS, depending on whether the STS measurement is performed in the centre or at the edge of the superlattice. This explains why the QW peaks after anneal of the Pb layer, are still rather broad for the lower coverages and become narrower for increasing coverage (Figure 3.8). Similar measurements on the as-deposited Pb layers reveal that at the corner holes and dimer rows no QWS are formed, as expected from the high incoherent backscattering explained in the above argument. The exact binding energy position of the states that are formed on the “flat” part of the 7x7 superlattice depends on how far away from the edge of this area the STS measurement is performed. This effect, combined with the rough growth front, will therefore lead to a substantial broadening of the QWS when measured with an area integrating technique like ARPES, as can be confirmed by the lineshapes of the peaks originating from the QWS in the layer in Figure 3.5.

From experiments performed by Aballe and co-workers¹⁹ and the data shown in Figure 3.25 it is clear that annealing of Al films both on Si(111)7x7 and graphite is necessary in order to obtain a defect-free film. Without a good crystalline structure, the coherent propagation of electron waves through the film is not possible. However, a similar anneal does not lead to a comparable width in QWS peaks on both substrates (Figure 3.27). This difference is primarily caused by the difference in interface structure. The interface of the annealed Al layers on Si(111)7x7 is completely incommensurate except for the growth direction²⁰, which means that the layer is fully relaxed towards its bulk lattice spacing. This results in a large number of different reflection conditions for the electrons approaching the interface; each of these conditions results in a different binding energy position of the QWS and altogether in a broadening of the measured QWS. Apart from this broadening for single layer heights, there is no clear indication that the resulting Al layers are atomically flat. A mixture of different heights may cause the already broadened QWS to overlap

18 I.B. Altfeder, V. Narayanamurti, and D.M. Chen, *Phys. Rev. Lett.* **88**, 206801 (2002).

19 L. Aballe et al, *Surf. Sci.* **482-485**, 488-494 (2001).

20 T.-M. Lu et al, *Phys. Rev. B* **39**, 9584 (1989).

and form an even wider peak. On the other hand, on the single crystal hexagonal graphite substrate the Al layers are decoupled from the substrate, resulting in perfect confinement conditions. Furthermore, these conditions are the same regardless of the exact location, which results in the sharp QWS peaks shown for this system in Chapter 3. Another consequence of the incommensurate interface between Al and Si(111) is that transmission of electrons across the boundary is highly improbable. The electrons thus experience a potential barrier due to the structural change, even when they have a binding energy in an energy region where states are present in the Si substrate. Therefore, QWS are also formed outside the silicon bandgap, in contrast to Pb/Si(111) where the interface forms a commensurate superlattice. As indicated in Section 3.1.1, features originating from a quantization of electrons are also observed outside the Si bandgap for Pb/Si(111)7x7 after annealing. These states are commonly referred to as quantum well resonances²¹ and are due to imperfect confinement conditions. That these states still experience some form of confinement is due to the presence of a very low potential barrier for the Pb/Si boundary, the quantum well system can thus be regarded as leaky at these energies.

For the Pb layers on Cu(111), the influence of the relative bandgap in the substrate is only visible in the layers deposited at low temperature. In Figure 3.3(a) no QWS are observed at binding energies larger than approximately 0.85 eV, which is the location of the band edge at the zone centre for Cu(111). The structure of the as-deposited layer is adapted to the lattice structure of the substrate, creating a situation where the electron wave functions of the Pb overlayer can match to those of the substrate outside of the relative gap. This structural arrangement of the interface is accompanied by the formation of a large number of defects, as shown by the presence of the bulklike feature originating from incoherent scattering as discussed above. Upon annealing the layer, this feature disappears (Figure 3.3(b)) indicating a structural rearrangement at the interface. The 30% lattice mismatch between Cu and Pb is too large for the formation of a superlattice, and the interface is incommensurate, strongly limiting the possibility of electron transport across it. Therefore, QWS are now observed outside the Cu(111) relative gap. On the other hand, the width of the QWS does not decrease much after anneal (Figure 3.4), due to the large number of non-equivalent reflection sites on the incommensurate lattice.

In conclusion, the interface can influence the formation of QWS in a metal overlayer in several ways. First, if the interface contains a large number of scatterers, incoherent backscattering prevails in these regions and only the Bloch wave function of the electrons remains, resulting in a bulk-like feature. Even a very smooth interface results in different reflection conditions, depending on the exact orientation with respect to the substrate atoms. These different conditions cause the QWS to have slightly altered binding energies, which in an area-integrating technique as PES results in a broadening of the measured QWS. Furthermore, when the interface is commensurate,

effective confinement only occurs within the bandgap of the substrate. For an interface where the lattice structure of the overlayer and substrate are largely independent of each other, the structural change also provides a potential barrier for the electrons, resulting in the formation of QWS. The structure of the interface can be strongly influenced by deposition temperature and post-treatment, and by the structure and characteristics of the surface before deposition. Si(111) $\sqrt{3}$ and graphite provide a perfect template for the deposition of Pb, because the optimal boundary conditions for the formation of QWS are created without further treatment of the layer. The difference between these two systems is that Pb/Si(111) $\sqrt{3}$ forms an almost perfect lattice match, whereas Pb/C(111) results in the formation of quasi freestanding Pb slabs.

4.3 Coupling of quantum wells: Pb/Al/Si(111)

All experiments presented so far in this thesis have been performed by depositing a metal on a bulk crystal. In the previous section I have shown that the interface properties between the overlayer metal and the substrate, together with the presence of electronic states in this substrate have a decisive influence on the formation of QWS in the overlayer. In the present section, results are shown for the situation where the substrate itself is composed of a metallic quantum well on a semiconductor substrate. This adds an additional interface to the system, whose properties may have a large influence on the formation of QWS. For example, for Ag layers on a thin layer of Au on Ag(111)²² it was found that QWS will only form in the Ag overlayer when the intermediate layer of Au has a thickness of 3 ML or more.

In order to achieve a double quantum well, first a 17 ML thick Al layer was prepared on Si(111)7x7 by low temperature deposition followed by annealing; the properties of such layers are well known, and therefore provide a good starting point. In the choice of overlayer material, it is important that the two metals do not intermix or form an alloy. Furthermore, the topmost layer should not require any additional treatment such as annealing, because this might destroy the layer underneath or cause intermixing. In this sense, Pb is the perfect choice of material; due to the size of both atoms Pb and Al will not form an alloy and Pb does also form well-developed layers at 100 K without further treatment, shown by the data for Pb/Si(111) $\sqrt{3}$ and Pb/graphite in this thesis. An additional advantage is that the electronic structure of Pb and Al shows strong similarities (Figure 2.13), and that Al has only one valence electron less than Pb.

Figure 4.9(a) shows the LEED pattern obtained after deposition of 3 ML of Pb on a 17 ML thick layer of Al on Si(111). The double inner spots originate from the Pb and the faint spots further to the outside are from the Al quantum well; due to the thickness of the Al layer the Si substrate spots

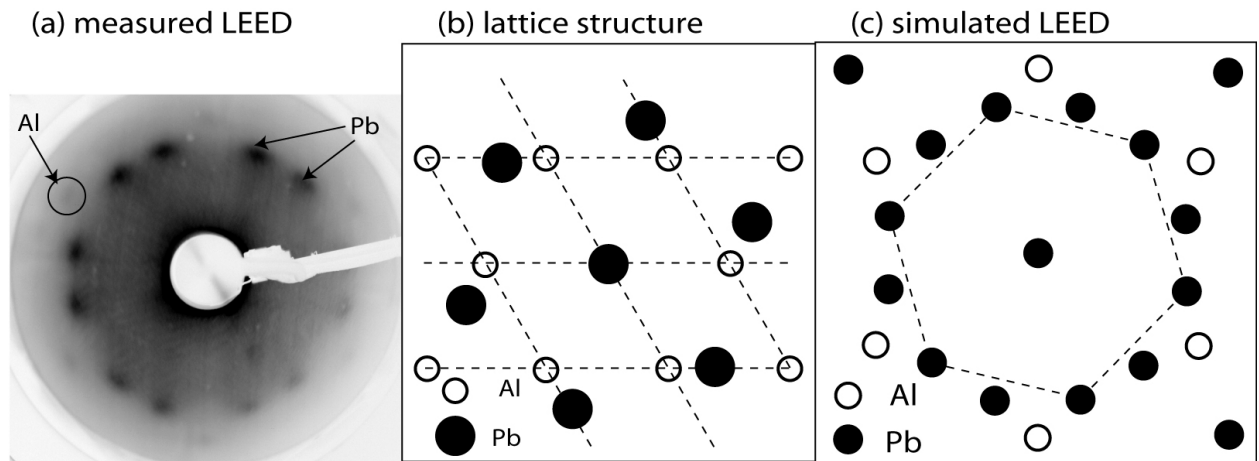


Figure 4.9: (a) Measured LEED pattern for 3 ML Pb on 17 ML Al on Si(111) obtained at an electron energy of 90 eV. (b) Suggested lattice structure for the same system for one domain. (c) Simulated LEED pattern for (b) and a second domain mirrored along the horizontal axis.

are not visible. The fact that two sets of hexagonal Pb spots are observed is an indication for the growth of two different domains of Pb on the single-domain Al overlayer. A measurement of the spacing of the centre of the Pb spots indicates that the two domains seem to be rotated 28° counter clockwise with respect to each other. However, a study of the lattice structure of both the Al(111) and Pb(111) layers indicates that the two Pb domains are rotated plus and minus 16° with respect to the Al lattice, and therefore 32° clockwise with respect to each other. The proposed interface lattice structure is schematically depicted in Figure 4.9(b) with the corresponding simulated LEED structure for two domains in Figure 4.9(c). In both images the bulk lattice spacing is used for both materials. In order to create a commensurate interface structure, I place the Pb atoms on the bridge sites of the Al surface. The same adsorption geometry may also be accomplished by mirroring the position of the Pb atoms along the horizontal axis, hence the two growth domains.

Normal emission angle-resolved photoemission spectra for a deposition series of Pb on 17 ML Al, acquired at two different photon energies, are displayed in Figure 4.10. These two photon energies were used because at 24 eV, Pb has a direct transition close to the Fermi level, and the photoemission cross section for the Pb valence states is at a maximum. The bulk plasmon of Al is located at a photon energy of 15 eV²³, which enhances the photoemission yield from Al layers by more than an order of magnitude. By using these two photon energies, it is possible to reach an at least qualitative “chemical sensitivity”, i.e. the possibility to distinguish between Al and Pb emission. This approach is necessary because at the beamline used, the Al 2p core level line is not accessible. The general trend at both photon energies is the same; upon increasing coverage, the number of QWS increases and they seem to move away from the Fermi level. From this behaviour, several indications about the growth mode can be determined. If the electrons were *not* able to

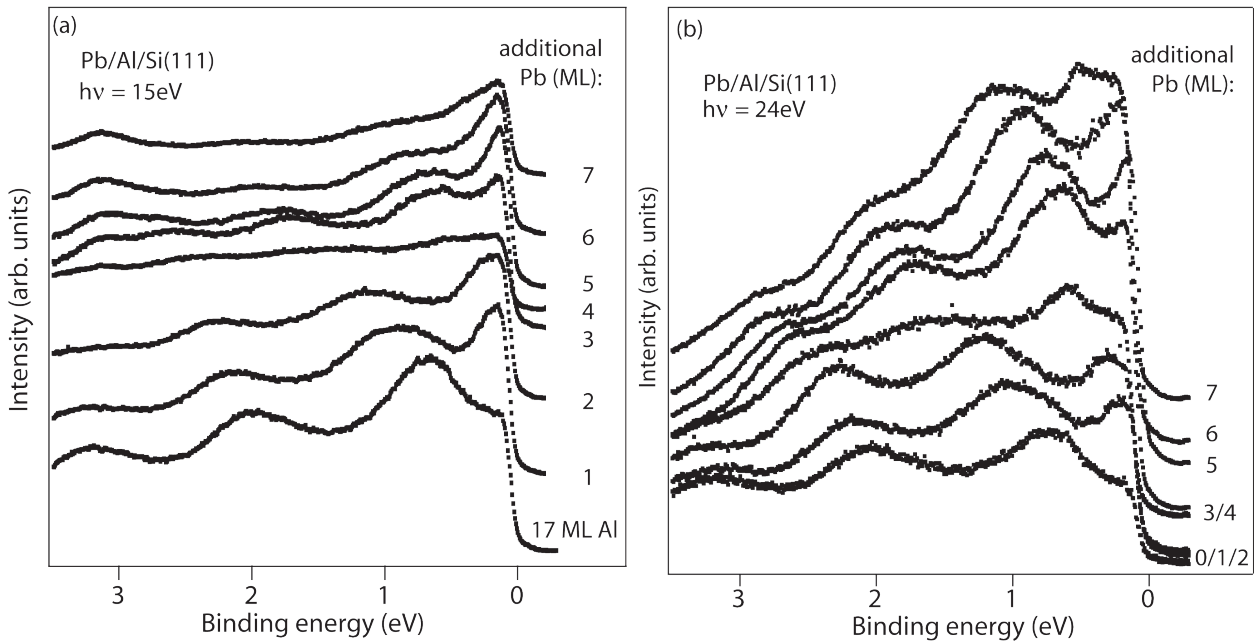


Figure 4.10: Energy distribution curves as a function of additional Pb coverage on a 17 ML thick Al film on Si(111)7x7 recorded at normal emission at a photon energy of 15 eV (a) and 24 eV (b). The QWS follow a gradual change in binding energy as a function of Pb coverage, indicating the formation of *one* quantum well.

cross the Pb/Al interface, the QWS were still expected to increase in binding energy after the initial Pb deposition. Since the Al/vacuum barrier is replaced with the lower Al/Pb barrier, this leads to a larger phase shift at this interface and an effective broadening of the quantum well, hence the QWS will move to higher binding energy. However, since only the interface is affected in this model, this effect should not continue for increasing Pb coverages, in contrast to the data shown here.

Without transmission across the Pb/Al interface, another option is the formation of a separate Pb quantum well on top of the Al quantum well. This would result in an initial motion of the Al QWS to higher binding energies due to the changing boundary conditions; for higher Pb coverages these states should remain at the same binding energy and additional Pb-derived QWS should appear at binding energies expected for these Pb layer thicknesses. From the gradual development of the QWS binding energies with increasing Pb coverage, and the regular spacing of the QWS, I conclude that this formation of two separate quantum well systems is not taking place here.

There are other possibilities than those described above: these are based on the traversing of electrons across the interface. An electron is allowed to cross the Pb/Al interface when its \mathbf{k} -vector is conserved and there are allowed states on both sides of the interface. For the commensurate Pb/Al interface described above, \mathbf{k} conservation is satisfied because inelastic scattering will be low. The bottom of the upper sp-valence band of both Pb and Al is located at 4.2 eV below the Fermi level; the lower bands do not match well, but they are not relevant in this study. The Fermi wavelength

(λ_F) in the (111) direction is 3.94 Å for Pb²⁴ and 3.6 Å for Al²⁵; the difference between these two is relatively small, considering the large lattice mismatch of 22 % between the two elements. This matching of λ_F and the bottom of the band indicates that the upper valence bands for both metals overlap almost exactly. Let us thus explore a model in which this overlap allows the two metal layers to form a matching quantum well with common energy levels. The allowed energy states at both sides of the interface are the same, and the electron can cross the interface between the Al layer and the additional Pb. I thus conjecture that the Pb/Al/Si(111) system can be regarded as one quantum well on a semiconductor substrate with an additional internal interface. Stated differently; Pb and Al form *one* metal layer with *one* valence band structure without alloying or intermixing.

Now on both sides of the interface, the electrons experience a different crystal potential, and the Bloch wavefunction will vary accordingly. Thus the complete electron wave function will have a shape as schematically depicted in Figure 4.11. The QWS envelope function does not change at the Pb/Al interface, whereas the rapidly oscillating Bloch wavefunction changes from a bulk Al state to one for bulk Pb. Photoemission spectroscopy only probes the top few atomic layers of the system, such that the final state and the matrix elements, for Pb coverages of 4 ML or more, therefore will resemble those dictated by the Pb Bloch wave. This is exactly what can be concluded from the data in Figure 4.10(b): the direct transmission envelope and the background strongly resemble the situation for layers only composed of Pb in Section 3.1.1. Moreover, the Al bulk plasmon will lose its effect on the photoemission intensity enhancement, resulting in the loss of intensity and contrast in Figure 4.10(a) for increasing Pb coverages.

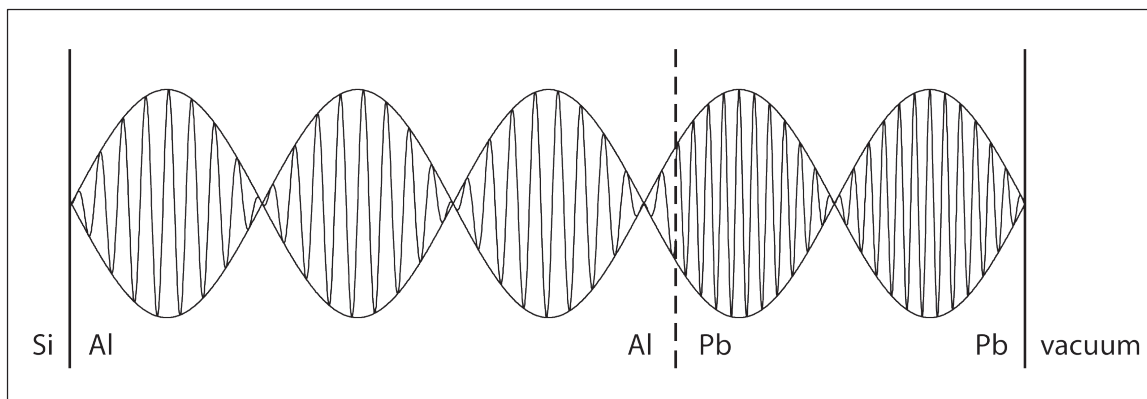


Figure 4.11: Electron wave function for the Pb/Al double quantum well. Due to the different lattice spacing, the Bloch wave changes at the interface, but the QWS envelope wave function is the same throughout the whole system. For simplicity the phase shift at the Si/Al and Pb/vacuum interfaces are not incorporated and arbitrary envelope and Bloch waves are displayed.

-
- 24 M. Jalochofski, H. Knoppe, G. Lilienkamp, and E. Bauer, *Phys. Rev. B* **46**, 4693 (1992); M. Jalochofski and E. Bauer, *Phys. Rev. B* **38**, 5272 (1988)
- 25 P. J. Feibelman, *Phys. Rev. B* **27**, 1991 (1983); P. J. Feibelman and D. R. Hamann, *ibid.* **29**, 6463 (1984).

In a photoemission experiment the layers will thus seem to become more Pb-like and less Al-like with increasing Pb coverage, while the character of the QWS is still largely influenced by the buried Al layer. This can be concluded from the fact that the apparent movement of the peaks is away from the Fermi level as is typical for Al, and not towards E_F as would be expected for Pb (see detailed description in Section 3.1). After deposition of 3 ML of Pb, the peak-to-valley ratio in the spectra has decreased dramatically, but recovers again for higher coverages, suggesting an improvement in layer structure has occurred. I assume that, at this coverage, part of the strain imposed on the Pb by the Al lattice is relieved, which results in a large amount of disorder at the interface and reduced transmission of electrons across this interface. For higher Pb coverages, both the Pb and the Al layer will experience some strain and the interface will be ordered again. Supporting evidence for the occurrence of a change in layer structure at a coverage of 3 ML Pb is provided by the development of QWS binding energy as a function of additional Pb coverage shown in Figure 4.12. Because of the better developed peaks, the QWS energies have been derived from the data obtained at $h\nu = 24$ eV, although they coincide with those derived from the 15 eV data. The lines in the image represent the slope of the QWS branches ($n - N$ is constant) at 2 and 6 ML of Pb, respectively, and after 3 ML the absolute value of the slope can be seen to increase. This is interpreted as being due to one of the remaining discrepancies between Al and Pb in the formation of quantum well states; Al can support a new QWS for approximately every 3 ML of additional coverage, and Pb for every second additional layer. For Pb coverages of more than 3 ML, the change in slope is rather gradual and will most likely level off at values expected for a Pb quantum well at higher coverages.

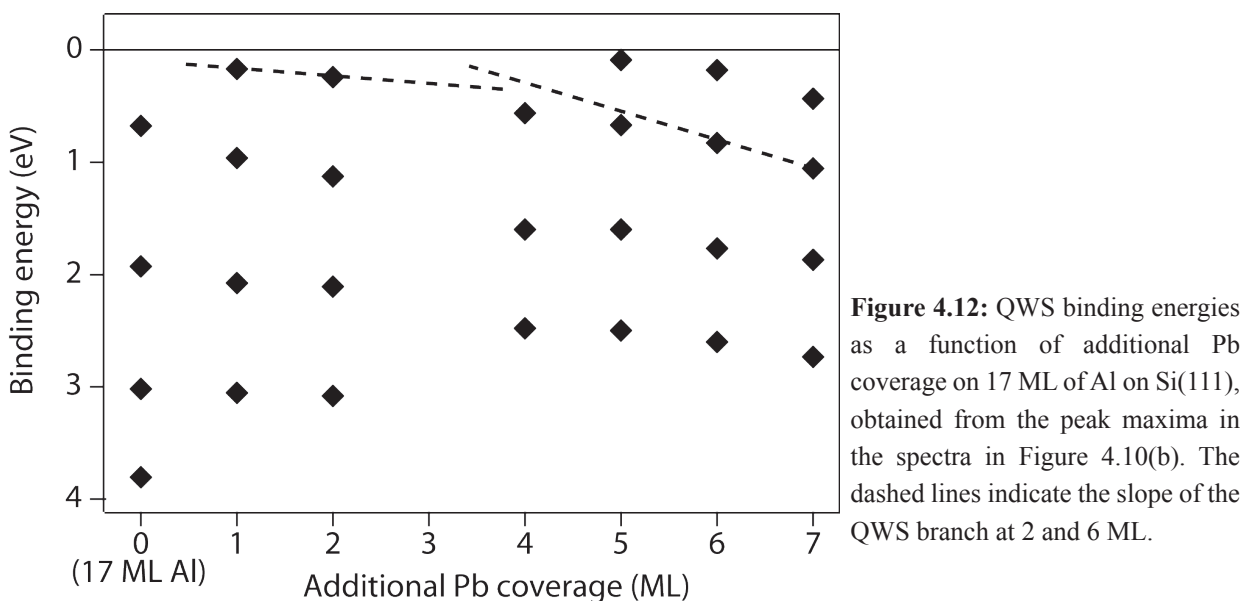


Figure 4.12: QWS binding energies as a function of additional Pb coverage on 17 ML of Al on Si(111), obtained from the peak maxima in the spectra in Figure 4.10(b). The dashed lines indicate the slope of the QWS branch at 2 and 6 ML.

In conclusion, the formation of a single metallic quantum well composed of layers of different metals is possible when a commensurate interface can be formed, and the bulk bands that will be quantized show a strong overlap. The QWS envelope function remains the same throughout the whole layer, but the Bloch wave function that is being modulated changes according to the metallic environment. The number of QWS that are formed per additionally deposited layer first depends on the initially deposited metal and gradually changes towards a value characteristic for the metal deposited on top. The rate of this change is likely to be guided by the relative fraction of the thicknesses of the two overlayers.

4.4 Hybridization of QWS with substrate bands

In Section 4.2 it was shown that effective confinement for a commensurate system is primarily achieved inside the band gap of the substrate. This discussion was limited to the centre of the SBZ, where the band gap is characterized by the position of the valence band maximum of the substrate. There is no reason to assume that this influence of the substrate bands will be limited to the situation for $k_{\parallel} = 0$. This section thus deals with the influence of the substrate bands on the QWS in the metal overlayer, extending beyond the influence of the band gap.

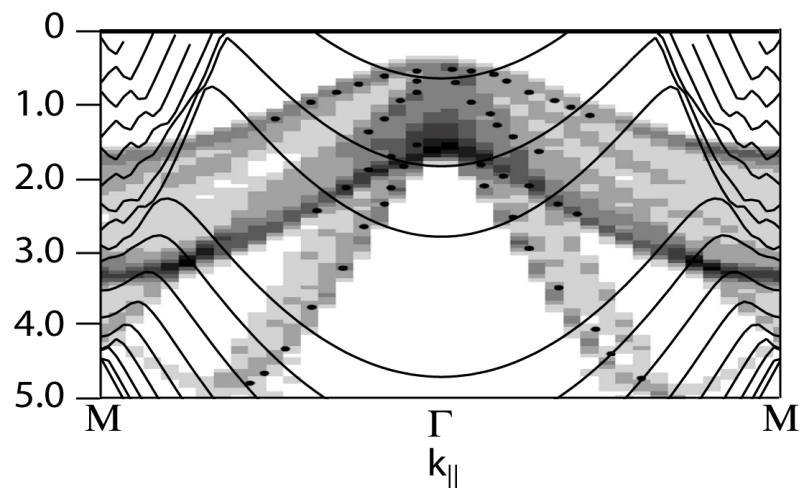


Figure 4.13: Si bulk band structure projected on the (111) surface from Ref. 26. Superimposed is the calculated band structure for a 9 ML thick free-standing layer of In.

Figure 4.13 shows DFT calculations for the projection of the Si bulk band structure onto the (111) surface²⁶. Superimposed on these data is the calculated electronic structure for a 9 ML thick free standing slab of In. There are many regions where the downward dispersing bands of the Si substrate and the upward dispersing In QWS coincide. At these locations, the interaction between the substrate bands and the QWS in the overlayer material is expected to be strongest.

The first experiment to clearly show that the substrate bandstructure leaves its mark on the electronic structure of the QWS was for Al on Si(111) by Aballe and coworkers²⁶. They observed that the Al QWS show a clear deviation from the expected behaviour when they cross the substrate bands. This was attributed to a singularity in the phase shift at the interface close to a band edge²⁷, due to a change in boundary conditions. When the phase shift shows a sudden change, this causes, according to Equation 1.2 and 1.3, an effective broadening of the quantum well, which in turn is reflected in the binding energy of the QWS. Therefore, by carefully studying the presence of kinks or other sudden changes in the QWS band structure, it is possible to identify the position of the bands in the substrate. The development of electron energy analyzers with high angular and energy resolution has intensified the search for any deviations from the expected behaviour of QWS close to a band edge. For QWS in atomically uniform Ag films on Ge(111), a gap was shown to open up at the location of the substrate band edge²⁸. Further ARPES studies for the same system²⁹ and for Mg on W(110)³⁰ have indicated a strong modification of the surface state due to the substrate bands. In both publications the authors suggest that the observed modification process is only possible for a surface state because of the imaginary part of the wave function, which is absent for QWS. Here I will show that this interaction can also be observed for *bulk-derived* QWS in In films on Si(111).

Figure 4.14 shows a cut through the surface Brillouin zone along the Γ -M direction for a 10 ML thick film of In on Si(111)7x7, obtained by joining several energy vs. angle photoemission images. In the region around $k_{\parallel} = 0$, three parabolic features with varying intensity can be observed, bordered on the higher binding energy side by a region with very low intensity. These features are the QWS derived from the $5p_z$ states in the upper valence band. The dark region is the fundamental band gap in bulk In where no QWS will form. Towards the edge of the SBZ the bands derived from the $5p_{x,y}$ states can be seen to disperse downward, and turn back again, after crossing the SBZ boundary. This is the same area in reciprocal space as shown in Figure 2.6, but for a different In coverage. The general trend of the QWS matches well to the calculated band structures for free standing In slabs, shown in Figure 3.15 and 4.13. There are, however, very clear deviations from the expected behaviour, especially in the regions where an interaction with the Si substrate band is expected. For the state marked as “QWS 2”, three different regions can be identified on each side of the zone centre; (1) the intense region close to E_F for $0.5 < k_{\parallel} < 0.65 \text{ \AA}^{-1}$, (2) a weaker region where the state has broadened for $0.3 < k_{\parallel} < 0.5 \text{ \AA}^{-1}$, and (3) a very low intensity region for $0 < k_{\parallel} < 0.3 \text{ \AA}^{-1}$. The boundary between those regions is defined by the points where the QWS crosses the projected band structure of Si from Figure 4.13.

27 M.A. Mueller, A. Samsavar, T. Miller, and T.-C. Chiang, Phys. Rev. B **40**, 5845 (1989).

28 S.-J. Tang, L. Basile, T. Miller, and T.-C. Chiang, Phys. Rev. Lett. **93**, 216804 (2004).

29 S.-J. Tang, T. Miller, and T.-C. Chiang, Phys. Rev. Lett. **96**, 036802 (2006).

30 F. Schiller, R. Keyling, E.V. Chulkov, and J.E. Ortega, Phys. Rev. Lett. **95**, 126402 (2005).

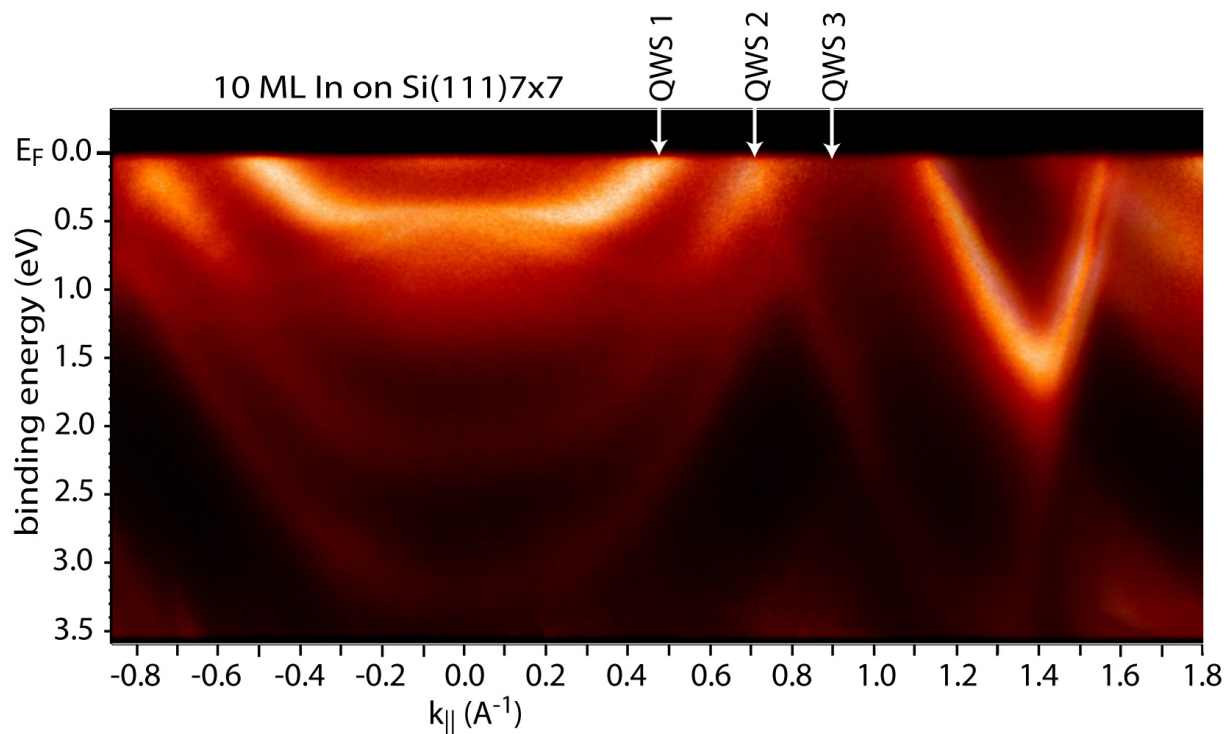


Figure 4.14: Cut through the SBZ along the Γ -M direction for a 10 ML thick layer of In on Si(111) obtained at a photon energy of 26 eV and a pass energy of 20 eV. The three QWS that are formed in the upper In valence band are indicated, for a further description of the features see text.

In Figure 4.15(a) the transition from region 1 to region 2 has been magnified by acquiring a closeup image with a lower pass energy (10 eV) and higher resolution. The contrast in the region of interest has been enhanced, leading to a saturation in the top left corner. The image has been inverted for clarity, black representing a high intensity and lighter colours a lower intensity. As a guide to the eye, the QWS is traced by a dotted line in both regions up to the point where it crosses the Si band. At this crossing point, the QWS state shows an abrupt change in binding energy from approximately 0.75 eV to 1.2 eV. This shift is rather unexpected, because on both sides of the crossing the QWS has the same quantum numbers. However, the observed shift in binding energy is readily explained by considering the change in boundary conditions upon crossing the Si substrate band. The presence of a high density of states in the substrate has two effects on the formation of QWS; first, the confinement barrier will be lowered, causing a less effective confinement, and thus blocking of QWS formation (see the comparison between Pb and Al in Section 4.2). This lower barrier is the reason that the intensity of the QWS suddenly decreases and the line width increases when moving from region 1 into region 2. The second effect of a high DOS in the substrate is that, for states that are still confined (as in Al and In), the tunnelling of electrons across the interface increases, effectively resulting in a wider quantum well. From Equation 1.2 it follows that the energy of the states with the same quantum number decreases, such that the binding energy increases. This energy shift of the QWS leads to a further observation: depending

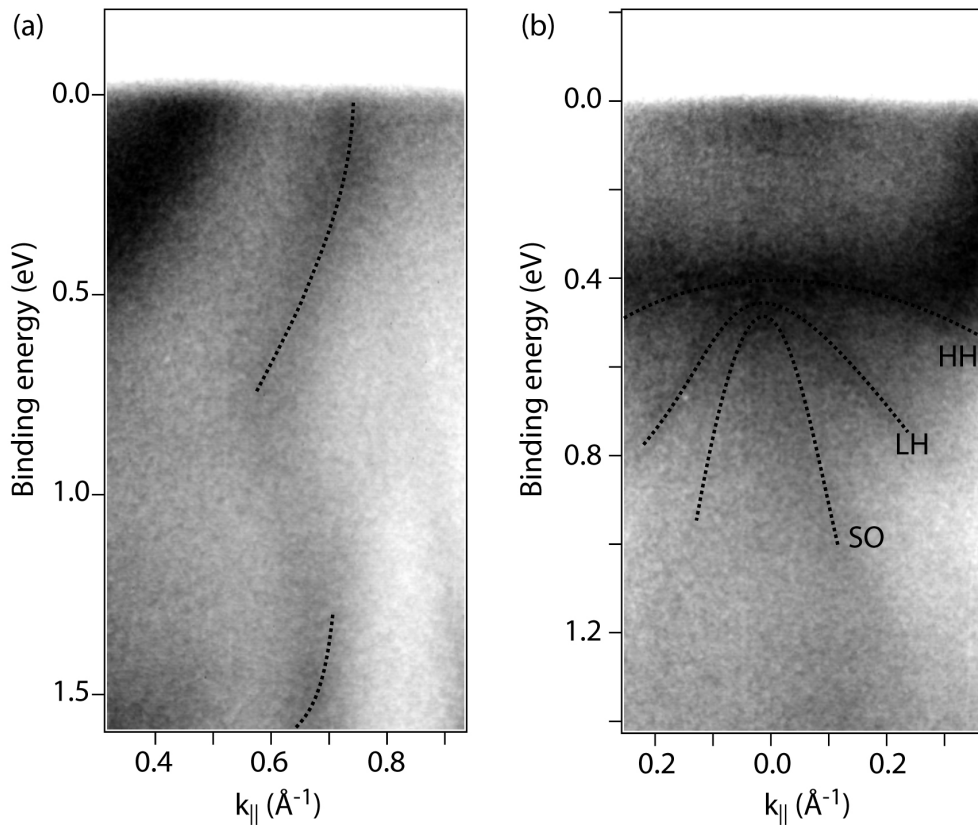


Figure 4.15: Close-up photoemission images of Figure 4.14 at (a) the point where QWS 2 crosses the Si substrate bands, and (b) around normal emission where QWS 1 hybridizes with the Si bands. Both images are obtained with a pass energy of 10 eV at a photon energy of 26 eV.

on whether the QWS approaches the Si band with increasing or decreasing $k_{||}$, the crossing point will shift from 0.72 \AA^{-1} to 0.59 \AA^{-1} . In the intermediate range, the QWS has two different binding energies for every $k_{||}$ value; a situation that seems to be contradictory to band structure theory. However, at the hybridization region of a sp-band with the d-bands in a metal crystal, this situation is commonly observed. In the present system it is rather unexpected, because the interacting bands do not belong to the same crystal.

At the transition from region 2 to region 3, the process described above is reversed. Here the QWS actually crosses into a region where the DOS in the substrate is low (Figure 4.13), leading to a lower phase shift and effective narrowing of the well. This will shift the QWS to lower binding energies. This upward movement relative to the energy in region 2 (Figure 4.14), can be easily verified visually. At present it is not clear why, with apparently better confinement conditions at the interface, the intensity of the QWS does not increase, but rather decreases further. In order to explain these details, full knowledge of the confinement barrier as a function of energy and $k_{||}$ is necessary. This knowledge can be obtained from calculations where the substrate is incorporated into the model. However, due to the lattice mismatch, these calculations are not possible with the current DFT code and this generation of computers.

The state identified as “QWS 1” in Figure 4.14 experiences a different influence of the substrate bands; at approximately $k_{\parallel} = 0.3 \text{ \AA}^{-1}$ the curvature of the QWS changes sign. S-p-bands with a negative curvature around $k_{\parallel} = 0$ are unexpected for metals, even under a situation of reduced dimensionality. A magnification of this area, obtained at similar conditions as Figure 4.15(a) is depicted in Figure 4.15(b); again, darker colours indicate a higher intensity. The kink at 0.3 \AA^{-1} is even more dramatic, due to the strong magnification in the energy direction. Around the zone centre, three downward dispersing features can now be discriminated, each with a different curvature. From a comparison to Figure 4.13, these bands can be identified as the heavy-hole (HH), light-hole (LH), and split-off (SO) bands of the Si substrate, and are marked accordingly. The observation of substrate features here has a totally different origin than, for example, in the data for In/Si(111) and Pb/Si(100) in Figures 3.22 and 4.5. For these data the substrate band structure is visible because the layer has not fully closed (Figure 3.22) or the coverage is very low (Figure 4.5); i.e. it is due to direct emission from the substrate. The direct emission from the substrate bands probed in these data, can be safely excluded because the layer has closed and is much thicker ($\sim 30 \text{ \AA}$) than the mean free path of a photoemitted electron at these energies ($\sim 5 \text{ \AA}$). The observation of the Si bands in Figure 4.15(b) is thus mediated by the QWS formed in the In overlayer. Typically, two non-interaction bands will show an anti-crossing behaviour and are allowed to hybridize³¹. This hybridization of the QWS and the substrate bands, explains why the QWS follows the substrate bands and transmits the electronic structure of the substrate through the In layer.

The data discussed above show that a strong hybridization to the substrate bands, leading to a clear visualization of these bands, is not limited to the surface states of a thin metal film, as has been argued by Tang *et al.*²⁹ and Schiller *et al.*³⁰ This hybridization of QWS to the band in the substrate can be used to determine the shape of such bands in their ground state. Normally such a direct measurement is not possible due to final state effects, but with this technique bands can be measured independently of their final state. The formation of atomically flat layers is not essential in these measurements as has been mentioned previously²⁸, under the valid assumption that the energy of the Si bands does not change with coverage once the Schottky barrier has fully developed. For a mixture of coverages, the individual QWS cannot be as well resolved as for flat layers, but the position where the interaction with the substrate bands takes place is the same for all QWS. In Figures 4.14 and 4.15 it is observed that the influence of the substrate bands primarily occurs in the region where a QWS in the overlayer film is expected, outside of this range the influence of Si bands is not visible. An ideal case would therefore be a mixture of coverages, such that at every energy and k_{\parallel} value a QWS is formed, but that these do not overlap. This way, the full substrate band structure could be measured all at once. The challenge in using this technique is to find a combination of substrate and overlayer material that results in the formation of QWS, and has the right interface conditions to allow for hybridization to occur. When the interface lattice is

commensurate, no QWS will form outside the substrate band gap, and the crossing with substrate bands is thus limited. For a rough interface the QWS are not well-defined and the coupling to the substrate band depends strongly on the exact scattering conditions. At the moment, the *a priori* prediction of the exact formation of QWS when a thin metal film is deposited on a substrate has been proven elusive. The dependence of the character and formation of QWS on the interface properties is very strong, and as shown in Section 4.3, sometimes a small change in interface conditions can lead to dramatic differences in QWS formation. However, the processes and measurements described in the present work bring the goal of predicting QWS behaviour within reach.

In summary, the interaction between QWS and substrate bands is characterized by two phenomena. First, the rapid change of phase shift at the interface when crossing from a region of low DOS to a region of high DOS, results in an energy shift of the QWS between these two regions. Depending on the shape of the substrate bands, this may result in the situation where, for one k_{\parallel} value, the QWS has two binding energy values. The second process is the anti-crossing and hybridization between a QWS and the substrate bands. This effect is especially strong towards the valence band maximum of a semiconductor substrate. Both phenomena can be used to measure the substrate band structure in the ground state. A correct choice of substrate and overlayer material is essential for this still developing measurement technique.